electronics

Article

A Study on Analysis Method for a Real-Time Neurofeedback System Using Non-Invasive Magnetoencephalography

Kazuhiro Yagi [1,2], Yuta Shibahara [3,*], Lindsey Tate [4] and Hiroki Tamura [4,*]

[1] Interdisciplinary Graduate School of Agriculture and Engineering, University of Miyazaki, Miyazaki 889-0921, Japan
[2] Department of Clinical Laboratory, Junwakai Memorial Hospital, Miyazaki 880-2112, Japan
[3] Sony Semiconductor Solutions Corporation, Atsugi 243-0014, Japan
[4] Faculty of Engineering, University of Miyazaki, Miyazaki 889-2192, Japan
* Correspondence: montre5005@gmail.com (Y.S.); htamura@cc.miyazaki-u.ac.jp (H.T.); Tel.: +81-985-58-7409 (Y.S. & H.T.)

Abstract: For diseases that affect brain function, such as strokes, post-onset rehabilitation plays a critical role in the wellbeing of patients. MEG is a technique with high temporal and spatial resolution that measures brain functions non-invasively, and it is widely used for clinical applications. Without the ability to concurrently monitor patient brain activity in real-time, the most effective rehabilitation cannot occur. To address this problem, it is necessary to develop a neurofeedback system that can aid rehabilitation in real time; however, doing so requires an analysis method that is quick (less processing time means the patient can better connect the feedback to their mental state), encourages brain-injured patients towards task-necessary neural oscillations, and allows for the spatial location of those oscillation patterns to change over the course of the rehabilitation. As preliminary work to establish such an analysis method, we compared three decomposition methods for their speed and accuracy in detecting event-related synchronization (ERS) and desynchronization (ERD) in a healthy brain during a finger movement task. We investigated FastICA with 10 components, FastICA with 20 components, and spatio-spectral decomposition (SSD). The results showed that FastICA with 10 components was the most suitable for real-time monitoring due to its combination of accuracy and analysis time.

Keywords: magnetoencephalography; continuous wavelet transformation; event-related desynchronization; event-related synchronization; independent component analysis; spatio-spectral decomposition

check for updates

Citation: Yagi, K.; Shibahara, Y.; Tate, L.; Tamura, H. A Study on Analysis Method for a Real-Time Neurofeedback System Using Non-Invasive Magnetoencephalography. *Electronics* **2022**, *11*, 2473. https://doi.org/10.3390/electronics11152473

Academic Editor: Yu Zhang

Received: 13 July 2022
Accepted: 29 July 2022
Published: 8 August 2022

1. Introduction

For diseases that affect brain function, such as Parkinson's disease and stroke, post-onset rehabilitation plays a critical role in the wellbeing of patients. Neurofeedback systems repeatedly collect neuroimaging data while participants process a stimulus or perform a task and then provide visual, auditory, haptic, or electrical feedback so that the participant can learn to modulate their own brain activity [1]. Many patients retain intact brain function, head, and eye movements, a significant number of approaches focus on methods based on brain activity. Such methods utilize electroencephalography (EEG) combined with eye movements using electrooculography (EOG) [2,3]. The relationship between EEG and eye movements has been well studied and is widely used in fields such as brain–computer interface and human-computer interface. One of the techniques used for non-invasive brain function evaluation is magnetoencephalography (MEG) [4,5]. MEG has high temporal resolution as well as high spatial resolution, and it is commonly used clinically for epilepsy diagnosis and rehabilitation [6]. However, without the ability to monitor and derive meaning from a patient's brain activity in real time during rehabilitative exercises, the most efficient rehabilitation cannot occur. Connecting a patient's brain activity to the calculated

feedback as quickly as possible is critical for achieving effective rehabilitation. It is known that recovery from rehabilitation involves a variety of normal activation patterns in the brain [4,7–9]. Our goal with this work was to develop an analysis method to evaluate brain function in real time by focusing on known, healthy, and task-necessary neural patterns.

Sensorimotor rhythms (SMR) are neural oscillations in the 8–30 Hz band that occur in the sensorimotor cortex [10]. SMR band rhythms may be more specifically around 13–15 Hz in most people [11]. Event-related desynchronization (ERD) and synchronization (ERS) are patterns in SMR that occur during real and imagined movement [12,13]. ERD is a time-locked decrease in SMR band spectral power, relative to baseline power in the same frequencies, during real or imagined movement, while ERS is a time-locked increase in SMR band spectral power immediately following the ERD [14]. Neither ERD nor ERS is phase-locked [15]. While both ERD and ERS have been observed over the entirety of the SMR band, ERD has often been observed in lower frequencies (alpha band 8–13 Hz, specifically the mu rhythm from 10–12 Hz) while ERS has been observed in higher frequencies (beta band 13–30 Hz). Due to the rapid occurrence and recovery of ERD and ERS—measurements can be taken in a fraction of a second [15]—these patterns are prime targets for feature extraction in a neurofeedback system, which must quickly analyze and return feedback to the patient. Individual differences have been observed in ERD and ERS frequencies [14], leading to the need for neurofeedback to be personalized on a patient-by-patient basis. Creating a neurofeedback system around ERD and ERS is advantageous to patients with paralysis because ERD and ERS are produced by both motor tasks (i.e., real physical movement) and motor imagery (MI; i.e., imagined or visualized movement without physically moving the body) [12,16,17].

Preliminary work on an MEG-based neurofeedback system to improve motor function [18,19] used data from healthy subjects performing a motor task to train an adaptive neural network classifier. However, these systems rely on the assumption that a machine learning model trained on data from healthy participants will be able to adapt to clinical use in rehabilitating patients. Although the researchers achieved an impressive 96.5% classification accuracy in their "pseudo-real-time" test using a single held-out subject's data [19], the assumption of applicability to patients may not prove dependable. While we agree with the reasoning of Halme and Parkkonen (2018) [18] that "when employing neurofeedback for rehabilitation, the feedback should drive brain activity towards that of a healthy brain and not to reinforce the prevailing pathological state as a patient-specific [brain-computer interface] might do," we differentiate between location of brain activity and event-related oscillatory patterns [18]. In patients with cortical lesions who leverage neuroplasticity to regain function, the location of activity may be altered from healthy brains and from other patients' brains [20,21], while the temporal and oscillatory patterns should remain the same if those patterns are functionally required for movement [19]. We propose the use of observations of timed oscillatory phenomena (i.e., ERD and ERS) from healthy participants to inform a motor-task-specific neurofeedback system for rehabilitating patients with paralysis as a result of brain damage. Furthermore, training a classifier during a calibration period at the beginning of a patient's neurofeedback session may inadvertently strengthen unhelpful activity if the patient is not able to immediately access healthy motor imagery (MI) or if their MI is weak. Finally, the classification of MI into specific categories (e.g., rest vs. MI) is potentially less useful for rehabilitation than a quantitative indicator of performance which might be able to be trained to increase in strength.

The purpose of this study was to investigate the use of MATLAB's spatio-spectral decomposition (SSD) algorithm and MNE-Python's FastICA algorithm for quick extraction of event-related desynchronization (ERD) and synchronization (ERS) information from real-time MEG during spontaneous movement [12,22–24]. SSD and FastICA are both techniques that have been used for decomposing data recorded from EEG/MEG into components each described by source location and time course. FastICA is a popular form of independent components analysis (ICA), which decomposes a signal by making use of the non-Gaussianity of the additive sources; in the case of FastICA specifically, this is

performed using skewness [22]. SSD, however, optimizes the signal-to-noise ratio (SNR) of neural oscillations by amplifying power in a specified frequency band while diminishing power in the flanking frequency bands [22]. SSD was chosen for this study due to its indication as the superior method for MI feature extraction from MEG data [18]. FastICA was chosen for this study for three important reasons: ICA is similar to SSD and has been compared to SSD in previous research [22]; to our knowledge, FastICA specifically has not been compared to SSD; and FastICA aims to shorten the often-lengthy analysis time of ICA algorithms. The processing time required to provide feedback to a patient is critical in neurofeedback; therefore, we seek to minimize processing time to 3 s or less between the end of an MI period and the presentation of feedback to the participant. SSD computes around 10,000 times faster than does ICA, and SSD is based on linear decomposition that does not assume non-Gaussianity [22]. For this preliminary research, MEG data was recorded from a healthy subject during spontaneous movement and analyzed offline using proposed techniques for real-time analysis in a neurofeedback system. Although SSD has been found to outperform SOBI ICA in reconstructing simulated data [22], we found that FastICA outperformed SSD in the task of quickly extracting ERD and ERS from real data. Due to its superior classification results, FastICA was chosen as the superior option for ERD and ERS feature extraction in a neurofeedback system.

In this paper, we develop an analysis method for a real-time neurofeedback system that enables more effective rehabilitation using non-invasive MEG. We force SSD, ICA as the superior method for MI feature extraction from MEG data. SSD was compared to ICA, specifically FastICA, run with both 10 and 20 components. Decomposition methods are compared in terms of analysis time and their ability to detect of ERD and ERS patterns. We discuss these results and provide recommendations for application of these results to motor-function rehabilitative neurofeedback systems.

2. Materials and Methods

2.1. Data Collection

The data were collected using full-head 306-channel magnetoencephalography (Vectorview, Elekta-Neuromag, Helsinki, Finland) at a sampling frequency of 1000 Hz. To reduce power supply noise and other interference, measurements were taken inside a magnetic field shield room (1 kHz shielding rate 55.2 dB). The participant was a healthy person who had an accelerometer attached to the middle finger of his right hand. Data from the accelerometer was used to record subject motor task execution. This protocol was approved by the Ethics Committee of the JUNWAKAI MEMORIAL HOSPITAL, Japan (protocol code 220629-1, on 29 June 2022).

Each of the 60 trials consisted of three parts: preparation, task, and rest (Figure 1). Visual cues were presented to the subject using a projector placed in front of the subject. First, the subject was given the Preparation cue. After a delay of 2.0 s, the subject was given the Go cue, at which they performed the motor task. Finally, the Rest cue was presented 3.0 s after the Go cue. Another Preparation cue was presented after 5.0 s of rest. The subject was instructed not to move during the preparation or rest periods. When the subject received the Go signal, they performed the motor task: self-initiated spontaneous flexion (i.e., bending) and extension (i.e., relaxing) movements of the middle finger of the subject's right hand (hereinafter referred to as the "task").

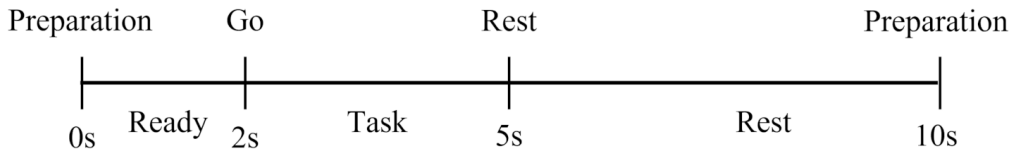

Figure 1. The flow of a single trial. There were 60 trials in total.

2.2. Analysis

After collecting the raw MEG data from all 306 channels, we selected all gradiometers (207 ch) then we repaired artifacts with Fast ICA or SSD. Finally, we assessed brain activity by calculating ERD and ERS.

2.2.1. ICA

Independent component analysis (ICA) is a technique for estimating independent source signals from a set of recordings in which the source signals were mixed in unknown ratios. Gradiometer data was bandpass filtered above 8 Hz and below 30 Hz in order to exclude signals and noise outside of the sensorimotor rhythm (SMR). MNE-Python was used to run FastICA analysis on the bandpass filtered gradiometer data. MNE is an open-source software supporting a collaborative development effort which provides a complete pipeline for MEG and EEG data analysis [25,26]. Because the ultimate application of this analysis will be within a neurofeedback system, processing speed was critical. Therefore, the specific ICA algorithm chosen for this analysis was FastICA, tested with the number of components set to 10 and 20. The FastICA analysis flow is depicted in Figure 2.

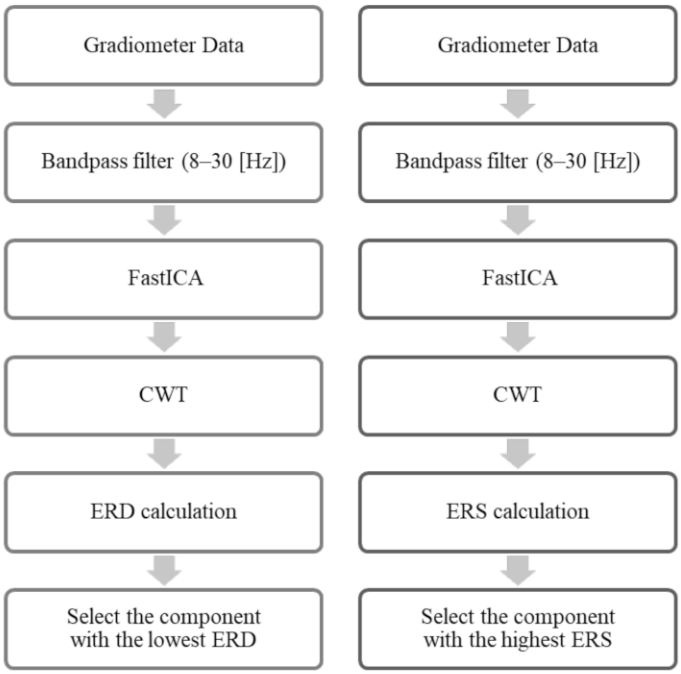

Figure 2. The FastICA analysis flow. Total number of components was 10 or 20.

2.2.2. ERD and ERS Calculation in ICA Components

We used event-related desynchronization (ERD) and synchronization (ERS) as indicators of task-relevant brain activity. ERD is a time-locked decrease in sensorimotor rhythm (SMR) band spectral power, relative to baseline power in the same frequencies, during real or imagined movement, while ERS is a time-locked increase in SMR band spectral power immediately following the ERD [18]. While both ERD and ERS have been observed over 8–30 Hz, ERD has often been observed in lower frequencies (alpha band 8–13 Hz) while ERS has been observed in higher frequencies (beta band 13–30 Hz). The same phenomenon has been reported to occur not only during actual exercise but also during motor imagery (MI) [27].

In order to calculate ERD and ERS, we used continuous wavelet transform (CWT) to obtain the power spectrum of the FastICA data for each frequency. The mother wavelet was "Morlet." Using the reference value calculated by averaging the data during the preparation period at a specific frequency, the rate of increase/decrease was calculated for all the data in one trial (Figure 3a, (1)). To calculate ERD, each frequency bin from 8 to 13 Hz was averaged,

first, during the reference period and, second, during the ERD period from 500 ms after the start of the task cue to 500 ms after the start of the rest cue (Figure 1: 2.5–5.5 s). This left one average value per frequency bin per time period. The reference values were subtracted from the ERD-period values, and the resulting number was divided by the reference value before being multiplied by 100 to derive the percent rate of change. The values were then averaged across frequency bins to leave one ERD value per component. The component with the lowest ERD value was selected as the ERD-representative component for that trial only (Figure 3c). A similar procedure was used to calculate ERS. The ERS period was from 500 ms after the rest start cue to 1500 ms after the rest start cue (Figure 1: 5.5–6.5 s), and the ERS frequency band was 13 to 30 Hz. However, ERS values were not averaged across the entire time and frequency ranges. Instead, the maximum rate of change was calculated, and the average across time and frequency was taken within a window of ± 1 Hz and ± 100 ms around the maximum point. If the maximum point was near a definitional time cutoff for ERS, the cutoff value was extended to accommodate the ± 100 ms window. However, frequency accommodations were not made outside of 8 to 13 Hz. ERS was calculated for each component. The component with the highest ERS value was selected as the ERS-representative component for that trial only (Figure 3d). The flow of the calculation of ERD and ERS in ICA components is depicted in Figure 3.

$$ROC = \frac{Data_{freq} - Reference_{freq}}{Reference_{freq}} \times 100 \quad (1)$$

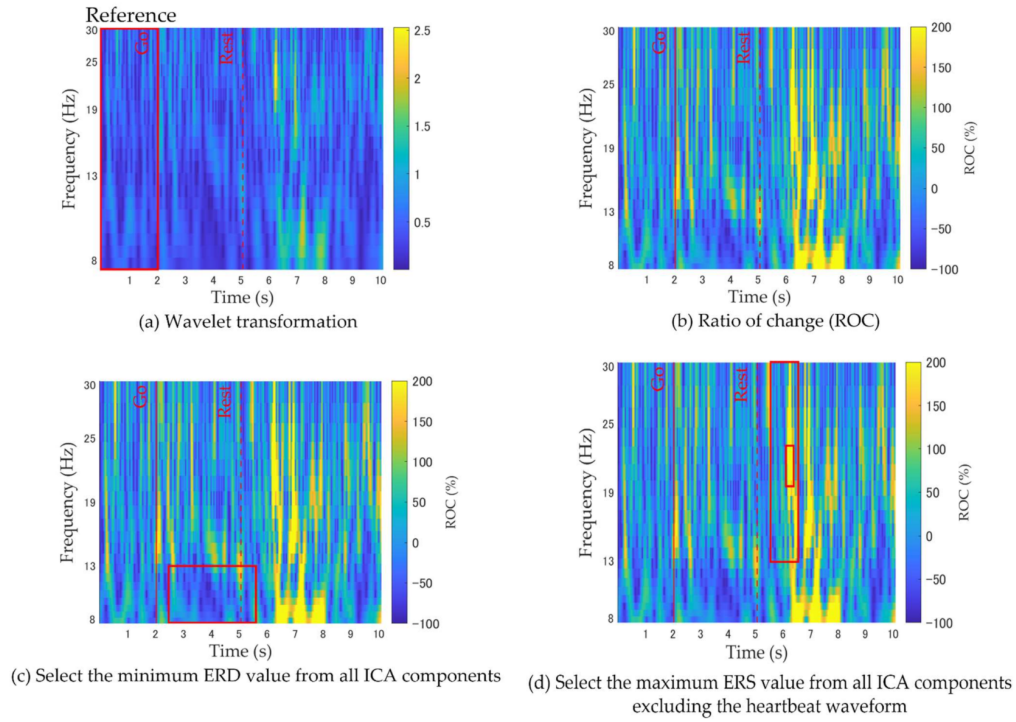

Figure 3. Flow of ERD and ERS calculation. (**a**) the wavelet-transformed data. (**b**) For the wavelet-transformed data, the rate of change from baseline (i.e., increase for ERS and decrease for ERD) was calculated using the average value from the reference period (from the preparation cue to the task cue). (**c**) ERD was calculated as the average rate (8–13 Hz) of decrease from 500 ms after the task cue "Go" until 500 ms after the rest cue "Rest". The component with the lowest ERD value was selected as the ERD-representative component for that trial only. (**d**) ERS was calculated as the average rate (13–30 Hz) of increase from 500 ms after the rest cue "Rest" until 1500 ms after the rest cue "Rest". The component with the highest ERS value was selected as the ERS-representative component for that trial only.

2.2.3. SSD

MEG signals contain overlapping activity from multiple neural sources as well as strong background noise. Spatio-spectral decomposition (SSD) is a novel method for fast extraction of neuronal oscillations which extracts neural oscillations within EEG/MEG data with a high signal-to-noise ratio. The SSD algorithm was applied to all gradiometer data for the extraction of alpha oscillations in the 8–13 Hz frequency band and beta oscillations in the 13–19 Hz frequency band. Figure 4 shows the SSD analysis flow.

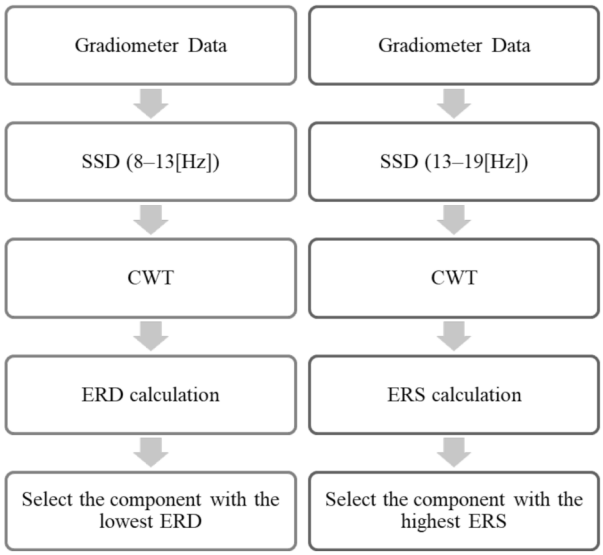

Figure 4. The flow of SSD analysis.

2.2.4. ERD and ERS Calculation in SSD Components

For the calculation of ERD and ERS, we used frequency ranges informed by both previous research as well as the data itself. The ERD range used in SSD analysis was 8–13 Hz while the ERS range used in SSD analysis was 13–19 Hz (Figure 3). Following the wavelet transform, the ERD and ERS results were calculated in the same way as the ERD and ERS calculations for ICA.

2.2.5. Classification

Two classification schemes were evaluated: (1) ERD change from baseline was less than −10.0% AND ERS change from baseline was greater than 150.0%; and (2) ERD change from baseline was less than the reference trial (i.e., Trial 31, which had no movement) AND ERS change from baseline was greater than the same reference trial. The cut-offs for the first classification scheme were derived from the data. The second classification scheme was developed in reference to the trial (Trial 31) wherein participant error led to no task performance following the Go cue; hypothetically, this trial should not have contained as much, if any, ERD and ERS patterns due to the lack of motor activity or MI.

3. Results

From this point onward, the results of ICA analyses will be labeled with the number of components used in the analysis (i.e., the analysis with 10 components will be indicated by "ICA_n10" while the analysis with 20 components will be indicated by "ICA_n20"). The results of the SSD analysis are labeled "SSD."

3.1. CWT Results

Example wavelet transforms of the ICA and SSD component data are provided (Figure 5). In each analysis, both ERD and ERS were indicated by one single component or by one component each. However, ERD and ERS patterns were not captured in all trials.

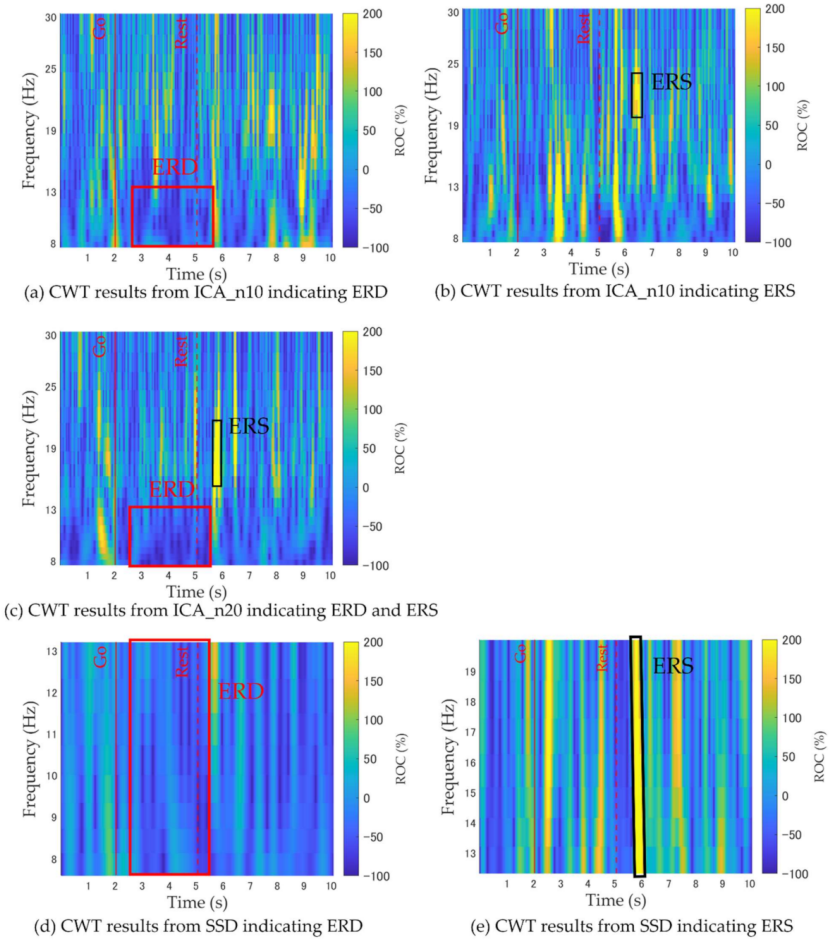

Figure 5. CWT results indicating ERD and ERS. (**a**) CWT results from ICA_n10 indicating ERD. (**b**) CWT results from ICA_n10 indicating ERS. (**c**) CWT results from ICA_n20 indicating both ERD and ERS in one component. (**d**) CWT results from SSD indicating ERD. (**e**) CWT results from SSD indicating ERS.

3.2. ERD/ERS Results

Figures 6–8 show scatter plots of the percent change in power from baseline for the ERD (*x*-axis) and the ERS (*y*-axis) for each ICA_n10, ICA_n20, and SSD. Each dot is an individual trial, with all 60 trials represented in each figure. The triangle represents the 31st trial where no task was executed after the Go cue (i.e., due to participant error, there was no movement execution).

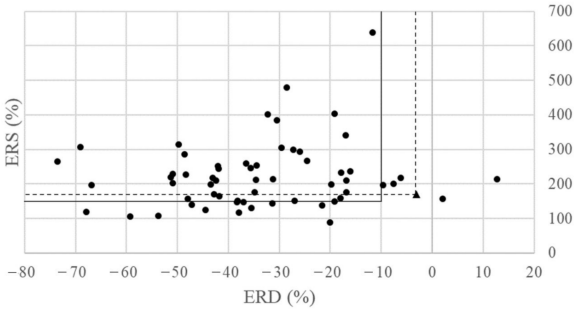

Figure 6. Plot of ERD ratio of change (*x*-axis) vs. ERS ratio of change (*y*-axis) derived from ICA_n10. Dotted lines indicate ERD/ERS criteria as set by session 31 (triangle). Solid lines indicate the criteria for ERD < −10% and ERS > 150%. The number that satisfies these criteria is the number of points in the upper-left section as demarcated by the respective lines.

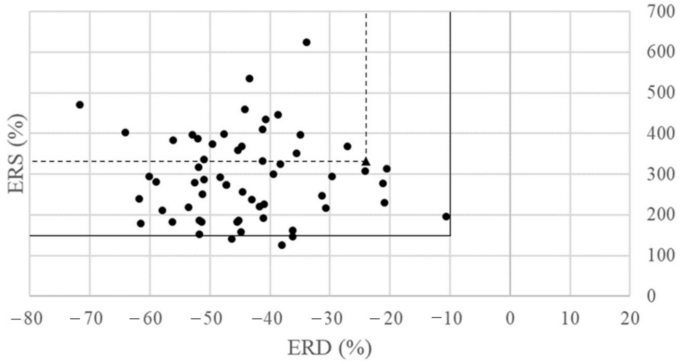

Figure 7. Plot of ERD ratio of change (*x*-axis) vs. ERS ratio of change (*y*-axis) derived from ICA_n20. Dotted lines indicate ERD/ERS criteria as set by session 31 (triangle). Solid lines indicate the criteria for ERD < −10% and ERS > 150%. The number that satisfies these criteria is the number of points in the upper-left section as demarcated by the respective lines.

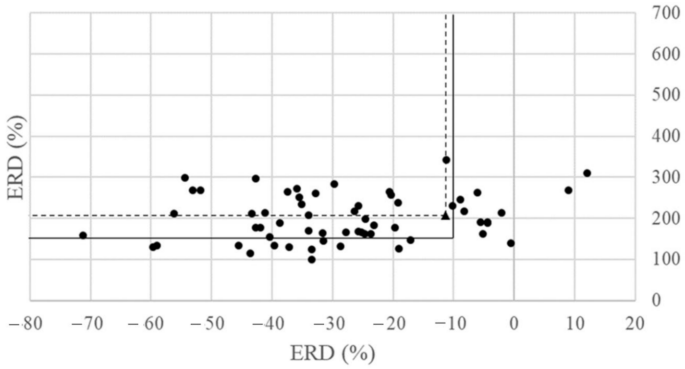

Figure 8. Plot of ERD ratio of change (*x*-axis) vs. ERS ratio of change (*y*-axis) derived from SSD. Dotted lines indicate ERD/ERS criteria as set by session 31 (triangle). Solid lines indicate the criteria for ERD < −10% and ERS > 150%. The number that satisfies these criteria is the number of points in the upper-left section as demarcated by the respective lines.

3.3. Classification Results

Table 1 summarizes the number of trials by decomposition analysis method that satisfies each of the two classification schemes. For the first classification scheme with data-derived cutoff values (i.e., ERD < (−10.0%) and ERS > 150.0%), the ICA_n20 method classified the most trials as showing ERD and ERS patterns (57 out of 60 trials or 95.0% of trials). For the second classification scheme with cutoff values derived from the no-movement trial, the ICA_n10 method classified the most trials as showing ERD and ERS patterns (39 out of 60 trials or 65.0% of trials).

Table 1. Number of trials (out of 60 total) that meet each condition.

	ERD < (−10%) and ERS > 150%	**|ERD| and |ERS| both > Trial 31**
SSD	37 (61.7%)	18 (30.0%)
ICA_n10	42 (70.0%)	39 (65.0%)
ICA_n20	57 (95.0%)	20 (33.3%)

3.4. Analysis Time

Analysis time from decomposition (i.e., ICA or SSD) through the ERD and ERS calculations was calculated for every trial and averaged by analysis method. The analysis time was estimated on a computer Core i7-7700k 4.2 GHz, 16 GB RAM, using Matlab2021b, Windows 10 Pro. The analysis time for ICA_n10 was 1.78 ± 0.68 s, ICA_n20 was 4.74 ± 0.89 s, and SSD was 1.97 ± 0.11 s.

3.5. Verification with a Second Participant

In order to confirm our results, we repeated the experiment with a second healthy participant and ran the same analyses. Results are presented in Table 2. FastICA with 20 components had the highest accuracy (98.3%) in detecting ERD and ERS patterns. FastICA with 10 components had the shortest analysis time (0.80–1.68 s).

Table 2. Method verification with test data.

	ERD < (−10%) and ERS > 150%	**Processing Time (s)**
SSD	39/60 (65.0%)	1.95 ± 0.15
ICA_n10	40/60 (66.7%)	1.24 ± 0.44
ICA_n20	59/60 (98.3%)	3.52 ± 1.58

4. Discussion

The purpose of this study was to develop an analysis method for a real-time neurofeedback system that enables more effective rehabilitation using non-invasive MEG. Spatio-spectral decomposition (SSD) was compared to independent components analysis (ICA), specifically FastICA, run with both 10 and 20 components. Decomposition methods were compared in terms of analysis time and their ability to detect of ERD and ERS patterns.

As shown in Figure 5, we observed increases and decreases in sensorimotor rhythm (SMR) frequency power that has previously been described as event-related desynchronization (ERD) and event-related synchronization (ERS). All three tested analysis methods were able to detect ERD and ERS as related to a finger movement task in two healthy subjects. However, these methods could not detect ERD or ERS patterns in every trial. Figures 6–8 show the summative ERD and ERS results for all trials collected from Subject 1. In these figures, the triangle indicated Trial 31, wherein the task was not executed due to participant error; however, it is worth noting that the detected ERD and ERS in Trial 31 were not remotely outside of the range of ERD and ERS detected in the other trials by ICA_n20 and SSD. This may indicate ERD and ERS patterns less extreme than those in Trial 31 are not actually movement-related; alternatively, this could indicate that a different neurological or muscular process inhibited the participant from executing the motor task (i.e., the participant had ERD and ERS but was otherwise inhibited from task execution). In order to distinguish between these possibilities, more non-movement data, with and without motor imagery (MI), needs to be collected and analyzed. The second subject, whose data was used for verification, did not have a similar failed-task trial to which we could compare.

For the first classification scheme with data-derived cutoff values (i.e., ERD < (−10.0%) and ERS > 150.0%), the ICA_n20 method classified the most trials as showing ERD and ERS patterns (57 out of 60 trials or 95.0% of trials for Subject 1, and 59 out of 60 trials or 98.3% of trials for Subject 2). However, ICA_n20 had the longest analysis time at about 3–5 s, which is not ideal for a neurofeedback system due to the desire to promote patient learning by connecting neural activity with feedback as closely in time as possible. Using the same classification scheme, ICA_n10 identified 42 out of 60 total trials (70.0%) as showing ERD and ERS patterns for Subject 1 and 40 out of 60 trials (66.7%) as showing ERD and ERS patterns for Subject 2. The ICA_n10 analysis time was less than about 2 s, which is reasonable for a neurofeedback system. SSD also had a fast analysis time of less than 2 s, but the classification accuracy was the lowest at 37 out of 60 trials (61.7%) for Subject 1 and 39 out of 60 trials (65.0%) for Subject 2. For the second classification scheme with cutoff values derived from the no-movement trial (i.e., Trial 31), the ICA_n10 method classified the most trials as showing ERD and ERS patterns (39 out of 60 trials or 65.0% of trials). ICA_n10 was inferior to ICA_n20 in accuracy using the first classification scheme, but it boasts a critically faster analysis time; therefore, we conclude that FastICA with 10 components is the most suitable for real-time feedback systems. Furthermore, the correlation between the ERD value at ICA_n10 and the ERD value at ICA_n20 shows a high positive correlation of

$R = 0.81$. Even in the case of ERS, we have confirmed that a positive correlation is shown with a correlation coefficient of $R = 0.73$. In our future work, it is necessary to verify the relationship with topography which indicates the site of brain activity.

Currently, there are various MEG analysis methods, but a method for analyzing and evaluating in real-time has not yet been established [6,28]. This method may be able to extract ERD and ERS features in order to evaluate the tasks performed by the subject in a relatively short analysis time. Future research will verify whether this method can be utilized with paralyzed patients due to the differences between the brain activity of healthy subjects and paralyzed patients [29]. This study will reveal the differences in ERD and ERS activity between healthy subjects and patients and will bring us one step closer to implementing real-time neurorehabilitation.

5. Conclusions

The proposed method may allow us to assess brain activity in less than 2 s by performing an analysis using FastICA with 10 components. Future research includes additional offline analysis with new participants, comparing Morlet wavelet to fast Fourier transform (FFT) [30,31], comparing successive decomposition index (SDI) [32] to our established methods, and testing the proposed method in a real-time neurofeedback system. The proposed design for our clinical neurofeedback system to assist in the rehabilitation of stroke patients does not require classification but rather a quantitative indicator of joint ERD and ERS activity as a patient's brain activity changes over time, which we believe can be derived by summing the absolute values of ERD and ERS activity observed in this study. We plan to use the quantitative indicator in a custom adaptive learning algorithm to encourage continuous improvement in patient performance. Ultimately, this line of research will lead to the development of a system for the rehabilitation of patients who cannot move their limbs freely due to brain injuries or diseases. Additional research, including that involving executive function, may help to extend the feasibility of neurofeedback systems and rehabilitative brain-computer interfaces [33–37]. Not only rehabilitation but also the EEG-based attention measuring method [30,31] have been proposed and are expected to be used in various fields.

Author Contributions: Data curation, K.Y.; Formal analysis, Y.S.; Methodology, L.T.; Project administration, K.Y.; Software, Y.S.; Supervision, H.T.; Writing—original draft, Y.S.; Writing—review and editing, L.T. and H.T. All authors have read and agreed to the published version of the manuscript.

Funding: This research received no external funding.

Institutional Review Board Statement: The study was conducted in accordance with the Declaration of Helsinki, and approved by the Ethics Committee of the JUNWAKAI MEMORIAL HOSPITAL, Japan (protocol code 220629-1, on 29 June 2022).

Informed Consent Statement: Informed consent was obtained from all subjects involved in the study.

Conflicts of Interest: The authors declare no conflict of interest.

References

1. Sitaram, R.; Ros, T.; Stoeckel, L.; Haller, S.; Scharnowski, F.; Lewis-Peacock, J.; Weiskopf, N.; Blefari, M.L.; Rana, M.; Oblak, E.; et al. Closed-loop brain training: The science of neurofeedback. *Nat. Rev. Neurosci.* **2017**, *18*, 86–100. [CrossRef] [PubMed]
2. Antoniou, E.; Bozios, P.; Christou, V.; Tzimourta, K.D.; Kalafatakis, K.G.; Tsipouras, M.; Giannakeas, N.; Tzallas, A.T. EEG-Based Eye Movement Recognition Using Brain–Computer Interface and Random Forests. *Sensors* **2021**, *21*, 2339. [CrossRef] [PubMed]
3. Huang, Q.; He, S.; Wang, Q.; Gu, Z.; Peng, N.; Li, K.; Zhang, Y.; Shao, M.; Li, Y. An EOG-Based Human–Machine Interface for Wheelchair Control. *IEEE Trans. Biomed. Eng.* **2018**, *65*, 2023–2032. [CrossRef] [PubMed]
4. Tecchio, F.; Zappasodi, F.; Tombini, M.; Oliviero, A.; Pasqualetti, P.; Vernieri, F.; Ercolani, M.; Pizzella, V.; Rossini, P.M. Brain plasticity in recovery from stroke: An MEG assessment. *NeuroImage* **2006**, *32*, 1326–1334. [CrossRef] [PubMed]
5. Paggiaro, A.; Birbaumer, N.; Cavinato, M.; Turco, C.; Formaggio, E.; Del Felice, A.; Masiero, S.; Piccione, F. Magnetoencephalography in stroke recovery and rehabilitation. *Front. Neurol.* **2016**, *7*, 35. [CrossRef]
6. Foldes, S.T.; Weber, D.J.; Collinger, J.L. MEG-based neurofeedback for hand rehabilitation. *J. Neuroeng. Rehabil.* **2015**, *12*, 85. [CrossRef]

7. Wilson, T.W.; Fleischer, A.; Archer, D.; Hayasaka, S.; Sawaki, L. Oscillatory MEG motor activity reflects therapy-related plasticity in stroke patients. *Neurorehabil. Neural Repair* **2011**, *25*, 188–193. [CrossRef]
8. Schaechter, J.D. Motor rehabilitation and brain plasticity after hemiparetic stroke. *Prog. Neurobiol.* **2004**, *73*, 61–72. [CrossRef]
9. Jurkiewicz, M.T.; Mikulis, D.J.; McIlroy, W.E.; Fehlings, M.G.; Verrier, M.C. Sensorimotor cortical plasticity during recovery following spinal cord injury: A longitudinal fMRI study. *Neurorehabil. Neural Repair* **2007**, *21*, 527–538. [CrossRef]
10. Blankertz, B.; Sannelli, C.; Halder, S.; Hammer, E.M.; Kübler, A.; Müller, K.R.; Curio, G.; Dickhaus, T. Neurophysiological predictor of SMR-based BCI performance. *Neuroimage* **2010**, *51*, 1303–1309. [CrossRef]
11. Arroyo, S.; Lesser, R.P.; Gordon, B.; Uematsu, S.; Jackson, D.; Webber, R. Functional significance of the mu rhythm of human cortex: An electrophysiologic study with subdural electrodes. *Electroencephalogr. Clin. Neurophysiol.* **1993**, *87*, 76–87. [CrossRef]
12. Halme, H.L.; Parkkonen, L. Comparing features for classification of MEG responses to motor imagery. *PLoS ONE* **2016**, *11*, e0168766. [CrossRef] [PubMed]
13. Salmelin, R.; Hari, R. Spatiotemporal characteristics of sensorimotor neuromagnetic rhythms related to thumb movement. *Neuroscience* **1994**, *60*, 537–550. [CrossRef]
14. He, B. *Modeling & Imaging of Bioelectrical Activity*; BioElectric Engineering book series; Springer: New York, NY, USA, 2005.
15. Pfurtscheller, G. EEG event-related desynchronization (ERD) and synchronization (ERS). *Electroencephalogr. Clin. Neurophysiol.* **1997**, *103*, 26. [CrossRef]
16. McFarland, D.J.; Miner, L.A.; Vaughan, T.M.; Wolpaw, J.R. Mu and beta rhythm topographies during motor imagery and actual movements. *Brain Topogr.* **2000**, *12*, 177–186. [CrossRef]
17. Miller, K.J.; Schalk, G.; Fetz, E.E.; den Nijs, M.; Ojemann, J.G.; Rao, R.P. Cortical activity during motor execution, motor imagery, and imagery-based online feedback. *Proc. Natl. Acad. Sci. USA* **2010**, *107*, 7113. [CrossRef]
18. Halme, H.L.; Parkkonen, L. Across-subject offline decoding of motor imagery from MEG and EEG. *Sci. Rep.* **2018**, *8*, 10087. [CrossRef]
19. Zubarev, I.; Zetter, R.; Halme, H.L.; Parkkonen, L. Adaptive neural network classifier for decoding MEG signals. *NeuroImage* **2019**, *197*, 425–434. [CrossRef]
20. Valkanova, V.; Eguia Rodriguez, R.; Ebmeier, K.P. Mind over matter—What do we know about neuroplasticity in adults? *Int. Psychogeriatr.* **2014**, *26*, 891–909. [CrossRef]
21. McDonnell, M.N.; Koblar, S.; Ward, N.S.; Rothwell, J.C.; Hordacre, B.; Ridding, M.C. An investigation of cortical neuroplasticity following stroke in adults: Is there evidence for a critical window for rehabilitation? *BMC Neurol.* **2015**, *15*, 109. [CrossRef]
22. Nikulin, V.V.; Nolte, G.; Curio, G. A novel method for reliable and fast extraction of neuronal EEG/MEG oscillations on the basis of spatio-spectral decomposition. *NeuroImage* **2011**, *55*, 1528–1535. [CrossRef] [PubMed]
23. Haufe, S.; Dähne, S.; Nikulin, V.V. Dimensionality reduction for the analysis of brain oscillations. *NeuroImage* **2014**, *101*, 583–597. [CrossRef] [PubMed]
24. Stefanou, M.I.; Baur, D.; Belardinelli, P.; Bergmann, T.O.; Blum, C.; Gordon, P.C.; Nieminen, J.O.; Zrenner, B.; Ziemann, U.; Zrenner, C. Brain state-dependent brain stimulation with real-time electroencephalography-triggered transcranial magnetic stimulation. *J. Vis. Exp.* **2019**, *150*, e59711. [CrossRef] [PubMed]
25. Gramfort, A.; Luessi, M.; Larson, E.; Engemann, D.A.; Strohmeier, D.; Brodbeck, C.; Goj, R.; Jas, M.; Brooks, T.; Parkkonen, L.; et al. MEG and EEG data analysis with MNE-Python. *Front. Neurosci.* **2013**, *7*, 267. [CrossRef] [PubMed]
26. Gramfort, A.; Luessi, M.; Larson, E.; Engemann, D.A.; Strohmeier, D.; Brodbeck, C.; Parkkonen, L.; Hämäläinen, M.S. MNE software for processing MEG and EEG data. *NeuroImage* **2014**, *86*, 446–460. [CrossRef]
27. Pfurtscheller, G.; Lopes Da Silva, F.H. Event-related EEG/MEG synchronization and desynchronization: Basic principles. *Clin. Neurophysiol.* **1999**, *110*, 1842–1857. [CrossRef]
28. Soekadar, S.R.; Witkowski, M.; Mellinger, J.; Ramos, A.; Birbaumer, N.; Cohen, L.G. ERD-based online brain-machine interfaces (BMI) in the context of neurorehabilitation: Optimizing BMI learning and performance. *IEEE Trans. Neural Syst. Rehabil. Eng.* **2011**, *19*, 542–549. [CrossRef]
29. Kauhanen, L.; Rantanen, P.; Lehtonen, J.A.; Tarnanen, I.; Alaranta, H.; Sams, M.; Foundation, I. Sensorimotor Cortical Activity of Tetraplegics During Attempted Finger Movements. *Biomed. Tech.* **2004**, *49*, 2–3.
30. Katona, J.; Ujbanyi, T.; Sziladi, G. Examine the effect of different web-based media on human brain waves. In Proceedings of the 8th IEEE International Conference on Cognitive Infocommunications, Debrecen, Hungary, 11–14 September 2017.
31. Katona, J. Examination and comparison of the EEG based attention test with CPT and T.O.V.A. In Proceedings of the 15th IEEE International Symposium on Computational Intelligence and Informatics, Budapest, Hungary, 19–21 November 2014.
32. Tariq Sadiq, M.; Yu, X.; Yuan, Z.; Aziz, M.Z. Identification of motor and mental imagery EEG in two multiclass subject-dependent tasks using successive decomposition index. *Sensors* **2020**, *20*, 5283. [CrossRef]
33. Wang, W.; Collinger, J.L.; Perez, M.A.; Tyler-Kabara, E.C.; Cohen, L.G.; Birbaumer, N.; Brose, S.W.; Schwartz, A.B.; Boninger, M.L.; Weber, D.J. Neural Interface Technology for Rehabilitation: Exploiting and Promoting Neuroplasticity. *Phys. Med. Rehabil. Clin. N. Am.* **2010**, *21*, 157–178. [CrossRef]
34. Grosse-Wentrup, M.; Mattia, D.; Oweiss, K. Using brain-computer interfaces to induce neural plasticity and restore function. *J. Neural Eng.* **2011**, *8*, 25004. [CrossRef] [PubMed]
35. Birbaumer, N.; Cohen, L.G. Brain-computer interfaces: Communication and restoration of movement in paralysis. *J. Physiol.* **2007**, *579*, 621–636. [CrossRef] [PubMed]

36. Ang, K.K.; Guan, C.; Chua, K.S.G.; Ang, B.T.; Kuah, C.; Wang, C.; Phua, K.S.; Zheng Chin, Y.; Zhang, H. Clinical study of neurorehabilitation in stroke using EEG-based motor imagery brain-computer interface with robotic feedback. In Proceedings of the 2010 Annual International Conference of the IEEE Engineering in Medicine and Biology, Buenos Aires, Argentina, 31 August–4 September 2010; pp. 5549–5552. [CrossRef]
37. Daly, J.J.; Wolpaw, J.R. Brain-computer interfaces in neurological rehabilitation. *Lancet Neurol.* **2008**, *7*, 1032–1043. [CrossRef]